Pure Appl. Geophys. 177 (2020), 703–721

https://doi.org/10.1007/s00024-019-02351-9

Pure and Applied Geophysics

Study of Generation and Underground Flow of Acid Mine Drainage in Waste Rock Pile in an Uranium Mine Using Electrical Resistivity Tomography

Matheus Felipe Stanfoca Casagrande,[1] César Augusto Moreira,[1] and Débora Andrade Targa[1]

Abstract—Mineral exploration is often associated with the generation of environmental liabilities, whose potential damages might imperil local water quality. An example of these environmental impacts is the acid mine drainage—AMD, caused by sulfides oxidation and production of acid and saline effluents. The analysis of critical areas with generation and spread of contamination plumes becomes more feasible due to the possibility to obtain geophysical models of water systems, especially to identify regions with accumulation of reactive minerals and preferential water flows. The rock-waste pile named BF-04 fits in this context of contamination, and it was studied based on the Electrical Resistivity Tomography technique, inversion models and isosurface models, providing conditions to recognize sulfide zones (> 10.1 mV/V), whereas chaotic high salt content underground flows, along several depths, were identified by low resistivity zones ($< 75.8\ \Omega$ m). The complex behavior of groundwater flow in this kind of artificial granular aquifer is caused by its granulometric and lithologic heterogeneities, and compacted material. In addition, the results reveled a substantial water infiltration from Consulta creek, however the most critic zones for AMD generation are located at shallow levels where the waste rock material is more exposed to atmospheric O_2 and meteoric water infiltration. The bedrock was not associated with significant low resistivity anomalies, which means that its contribution to AMD generation was considered relatively less important. The results will contribute to the environmental remediation management and also to demonstrate the potential applicability of geophysical methods in mining wastes.

Keywords: Sulfides, contamination, aquifer, DC resistivity, induced polarization.

1. Introduction

Mineral industry has a historical role in the development of human communities around the globe, especially base industries that provide raw materials sources for other technological processes. The exploration of these mineral ores has a high potential to cause severe damages to the environment due to large waste and tailing piles, which demand proper studies to manage their disposal according to environmental law regimes. These laws aim to preserve the integrity of physical aspects and the welfare of human communities that live near mining complexes.

Mining sites, mainly the abandoned ones, also decrease the quality of superficial and underground drainage systems. Acid mine drainage—AMD is considered one of the worst environmental concern related to mining activities, whose phenomenon is caused by the exposure of sulfide minerals, previously isolated in the natural geological formation, to oxidizing environment. An acid environment is formed because of a decreasing of pH caused by the mineral oxidation into SO_4^{2-}, producing sulfuric acid in contact with water. As a result, the acid environment increases the mobility of heavy metals and the concentration of SO_4^{2-}, promoting soil, sediments and water degradation (Pichtel and Dick 1991; Blowes 1997; Campaner and Silva 2009).

This kind of environmental liability is globally distributed and its presence is attributed to the lack of strict statutes and clear regulations to establish how to prevent AMD and the mining industries duties towards environmental impacts (Naidoo 2017).

The AMD phenomenon is chemically formed by the oxidation of pyrite (FeS_2), one of the most common sulfide minerals associated with mineralized zones, followed by the precipitation of iron hydroxides and production of sulfate ions and acid solutions

[1] Geosciences and Exact Sciences Institute (IGCE), São Paulo State University (UNESP), 24-A avenue, 1515, Bela Vista, Rio Claro, São Paulo 13506-900, Brazil. E-mail: mfs-casagrande@hotmail.com; moreirac@rc.unesp.br; debora.targa@gmail.com

(H^+), as exemplified in the global chemical reaction (Lowson 1982; Akcil and Koldas 2006):

$$FeS_2 + 15/4O_2 + 7/2H_2O \leftrightarrow Fe(OH)_3 + 2SO_4^{2-} + 4H^+. \quad (1)$$

Acid mine drainage is often associated with waste and tailing piles of mineral industries, whose occurrence is narrowly related to the rock mineralogy (presence of reactive minerals, as sulfides), climate/humidity and oxygen availability. Based on these conditions, each contaminated site is unique considering the combination of these factors and the degradation level of the natural environment. Besides, the high potential for heavy metal mobility could also be a risk for human health and a threat to hydrological systems (Gray 1997; Pastore and Mioto 2000; Akcil and Koldas 2006).

Impacted hydrogeological sites present high concentration of chemical species dissolved in groundwater systems, which provide condition to quantify the environment electrical resistivity, once the electrolyte concentration is inversely proportional to this physical parameter (Merkel 1972; Yuval and Oldenburg 1996). Based on this principle, DC Resistivity method is considered an efficient geophysical tool in hydrogeological and environmental studies, usually associated with conventional techniques, as monitoring wells sampling and chemical analysis (Benson et al. 1997; Bermejo et al. 1997; Moreira and Braga 2009; Belmonte-Jiménez et al. 2012; Delgado-Rodriguez et al. 2014; Veloso et al. 2015; Moreira et al. 2017).

Another geoelectrical method widely applied in this kind of studies is the induced polarization (IP). Commonly used on mineral resources exploration, IP is based on the electrical polarization phenomenon, whose intensity is expressively higher in the presence of metallic minerals (Yuval and Oldenburg 1996; Campbell and Fitterman 2000; Campbell and Beanland 2001). Sulfide minerals accumulation exposed to specific humidity and oxidizing conditions plays an important role in acid effluent generation, and its identification and characterization can contribute to subsidize mitigation programs as a complementary tool.

The integration between these two geophysical methods is an alternative to study environmental impacts and tailing/waste piles produced by mineral industries, especially to identify sulfite zones, AMD sources, and underground flow patterns of saline effluents within waste piles of uranium mines (Power et al. 2018).

In view of environmental disasters that recently occurred in Brazil and their high potential for social-environmental impacts upon communities, these episodes demonstrated how monitoring and stability studies are important to preserve mining infrastructures as waste piles and tailings dam (Freitas et al. 2016; Lacaz et al. 2016; Lopes 2016). Such studies are only one of the many possibilities to apply geophysics on environmental survey, even though few studies have been published compared to other geophysics paper research.

Therefore, this paper aims to analyze the relationship between AMD origin and its flow within waste-rock piles at an unoperational uranium mine, as an attempt to comprehend physical processes and phenomena behind AMD generation. Thus, it will be possible to suggest technical procedures to mitigate environmental impacts in aquifer systems. The study is based on the integration between DC Resistivity and Induced Polarization methods to produce 2D tomographic and models generated by data interpolation.

2. *Study area and Characteristics of the Environmental Liability*

The study area consists on a waste-rock pile (BF-04) that belongs to Osamu Utsumi Mine (OUM), which is part of the Poços de Caldas mining site under Brazilian Nuclear Industries (Indústrias Nucleares do Brasil—INB) responsibility (Fig. 1).

This mining complex is located at the southeast portion of the Poços de Caldas alkaline complex, a region known as Cercado Field, which is part of Caldas city, Minas Gerais, Brazil. Uranium exploration started in 1981 as an open pit mine and, after 15 years, the uranium mining and milling operations have ceased, in 1995. Nowadays, the Osamu Utsumi Mine is at decommissioning stage and environmental recovery process.

The geological context of Osamu Utsumi Mine is related to polycyclic intrusions of alkaline rocks that

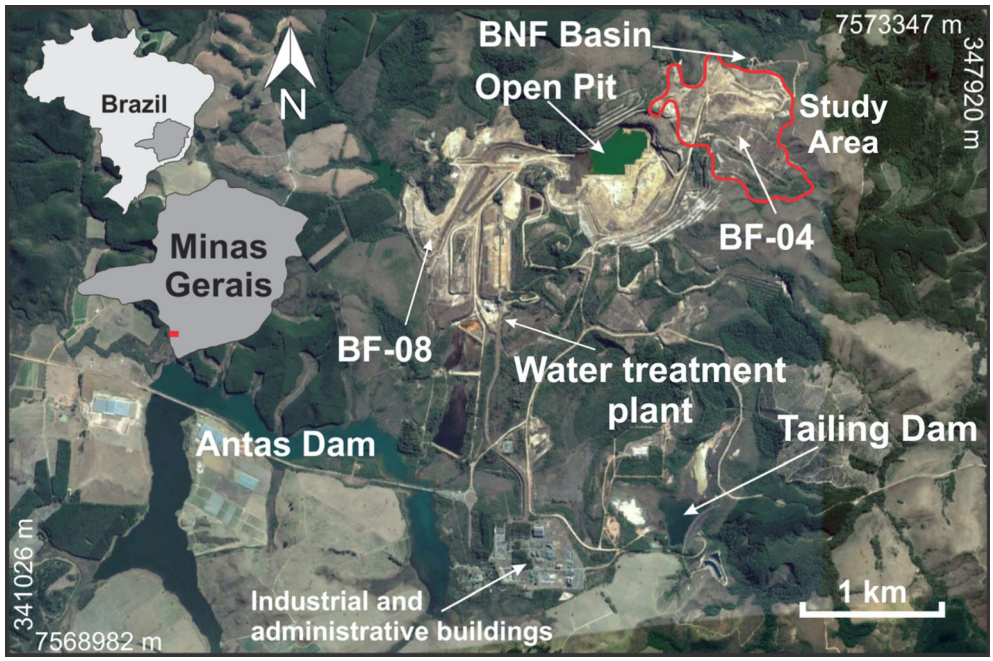

Figure 1
Osamu Utsumi Mine location, delimitation of BF-04 waste-rock pile and other compounds of the mining complex

compose the Poços de Caldas alkaline complex, a circular structure with 35 km of diameter and area of 800 km^2. The current morphology is product of erosion processes that excavated the caldera, whose oldest intrusions dated around 80 Ma (Fraenkel et al. 1985; Holmes et al. 1992; Moraes and Jiménez-Rueda 2008; Thedeschi et al. 2015).

BF-04 waste-rock pile was built at the northeastern portion of the industrial complex where the Consulta creek's valley was grounded, according to the end-dumping construction method. In order to inhibit water infiltration into BF-04, the natural stream was diverted to the pile's sides and the water flow was channeled towards River Verde. In addition, a layer of clay was disposed at the top of the pile to create a waterproof barrier to avoid water infiltration.

It was necessary to build a catchment basin at the upstream area and at base of the main pile slope to catch the acid and saline water that emerges from BF-04, named as BNF Basin (see Fig. 1). This structure aims to guarantee the quality of River Verde watershed, due to the high toxicity of heavy metals present in impacted effluents by AMD, as well as the presence of several radionuclides of ^{235}U, ^{238}U and ^{232}Th decay series. Contaminated water that reaches the basin system is pumped to water treatment plant where hydrated lime is added for neutralization. The chemical waste produced along this process is mostly composed by calcium diuranate with U_3O_8 and rare earth elements oxides at a grade of 0.25% and 2.5%, respectively, disposed inside the open pit mine.

BF-04 has an area of 56.4 ha and volume of 14.26 million m^3 whose material is composed by rocky waste that varies from clay to metric blocks provided by uranium exploration. Its chemical composition is mainly silicate minerals enriched in potassium and aluminum (54% de SiO_2, 22% de Al_2O_3 e 12% de K_2O) (Leite 2010), mineralogy compatible with nepheline syenites rocks intensely weathered and exposed to metasomatic processes (Table 1).

3. *Structure and Hydrochemical Aspects of the Hydrogeological System of BF-04*

Waste-rock piles work as granular aquifer systems, becoming part of the local geological setting even though they are artificially built and disposed on

Table 1

Mineralogical composition of BF-04

Mineral	Concentration in BF-04 (%)	
	Franklin (2007)	Leite (2010)
$BaSO_4$ (Barite)	2.00	–
FeO(OH) (Goethite)	2.00	6.37
SiO_2 (Silica)	0.01	–
$Al(OH)_3$ (Gibbsite)	1.25	2.50
Fe_2O_3 (Hematite)	1.5	–
Fe_2O_4 (Magnetite)	0.5	–
FeS_2 (Pirite)	2	–
UO_2 (Uraninite)	0.12	–
$Al_2Si_2O_5(OH)_4$ (Kaolinite)	20.00	34.79
$KAlSi_3O_8$ (K-feldspar)	50.00	54.85
CaF (Fluorite)	0.42	–
MnO_2 (Pyrolusite)	0.17	–
$KAl_3Si_3O_{10}(OH)_2$ (Muscovite)	20.00	2.12

the terrane. The BF-04 was disposed on a fractured aquifer system composed by potassic rocks, whose fracture system has a preferential strike to NE–SW with dip direction to NW and to NW–SE with dip direction both to NE and to SW (Targa et al. 2019). At the top of the pile, the material works as a phreatic aquifer vulnerable to local climate conditions, with a humid period between October and March when 80% of annual precipitation occurs, comprising a total volume of 1700 mm (Holmes et al. 1992; Cipriani 2002). Based on the local annual precipitation history and water discharge measurements at the catchment basin BNF, the residence time of water in the BF-04 hydrogeological system varies from 2 to 3 months, assuming no groundwater contribution from the underlying fractured aquifer, according to Fagundes (2005). Figure 2 shows elements that compose the BF-04 area (Fig. 2a), as well as a schematic model of groundwater flow through pile-basement system, whose direction is towards upstream of BNF catchment basin (Fig. 2b).

BF-04 has an anisotropic structure due to its construction method and the granulometric and compositional aspects of waste material. According to fieldwork observations, it is possible to notice evidences of particles segregation caused by gravitational process as the material had been disposed of following the end-dumping method (Fig. 3). Heavy vehicles traffic during the pile construction also promoted different stages of compaction along the several layers of waste material (Fala et al. 2003; Anterrieu et al. 2010).

This internal structure provides important hydrologic characteristics that control the generation and transport of AMD, mainly by controlling atmospheric air (through convective, advective and defuse movements) availability, and water flow throughout the waste material (Fala et al. 2003). The presence of compacted layers and fine-grain material accumulation tend to create saturated zones, once hydraulic conductivity (K_s) is directly proportional to the average grain size of the material that composes the hydrogeological system.

Historical chemical analysis of BF-04 groundwater quality shows different levels of AMD contamination, from extremely acid and saline effluents to neutral and natural water flows. An example of these divergent results is two piezometers installed at BF-04, Pz 03 and Pz 04 (Fig. 4). The first one showed critical results related to AMD, with pH of 3.5, average conductivity of 9.853 µS/cm and high concentration of SO_4^{2-} (22.000 mg/L), being installed about 420 m from Pz 04, whose analysis indicated waters with pH of 6.2, conductivity of 158 µS/cm and 16.4 mg/L of SO_4^{2-} (Franklin 2007; Alberti 2017). The variability of groundwater quality is another evidence of the complex underground flow pattern within the waste pile, as well as sulfide mineralization and AMD generation zones.

As BNF catchment basin receives all water flows from BF-04, its hydrochemical parameters have intermediate values, with pH around 4.2, conductivity of 1.297 µS/cm and sulfate concentration of 944 mg/L (Alberti 2017).

4. Methods and Data Acquisition

Many of geophysical methods are based on the quantification of voltages or magnetic fields associated with subsurface electrical currents, which may occur naturally through hydrogeological flow, oxidation–reduction processes or variations of magnetic field in the atmosphere or ionosphere (Milson 2003). DC resistivity method measures the electrical

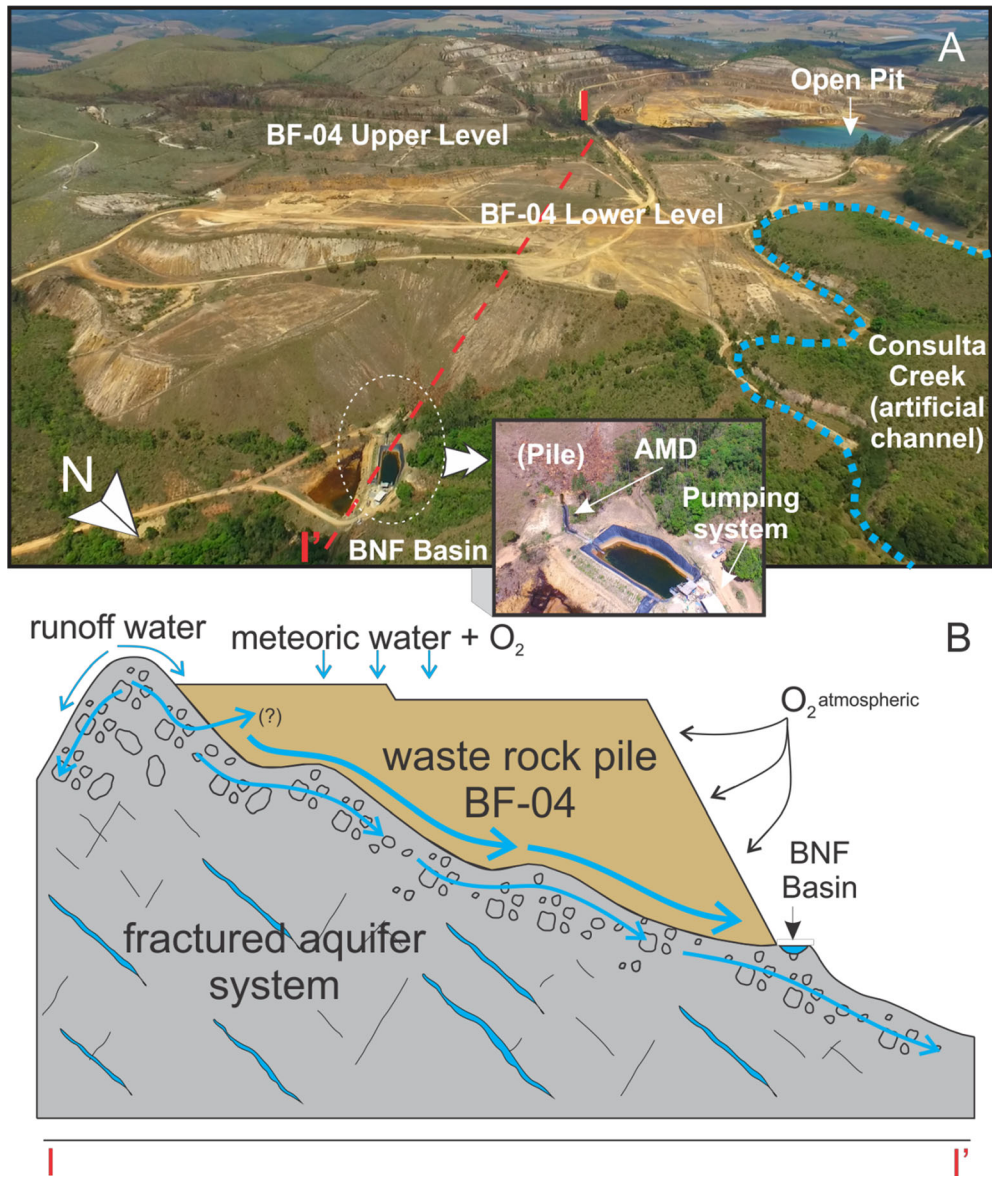

Figure 2

a BF-04 and surrounded areas with schematic section of the local hydrogeological system, with a rock basement (fractured system) under BF-04 (granular aquifer system). **b** schematic groundwater flows towards the BNF basin and their interaction with O_2 through the main slope

resistivity of geological environments, characterized by the difficulty of electric current propagating through a material considering its nature and physical condition. This geophysical method is based on the introduction of artificially-generated electric currents into the ground that results in potential differences measured at the surface (Mussett and Khan 2000; Kearey et al. 2002).

IP method is based on the polarizability effect associated with a physical phenomenon that occurs after the delay of artificial electric field stimulation in soils and rocks. Chargeability is a physical parameter intrinsic to geological materials, as metallic sulfides, graphite, oxides, clay minerals and water with high salt content, whose measurement can be done by

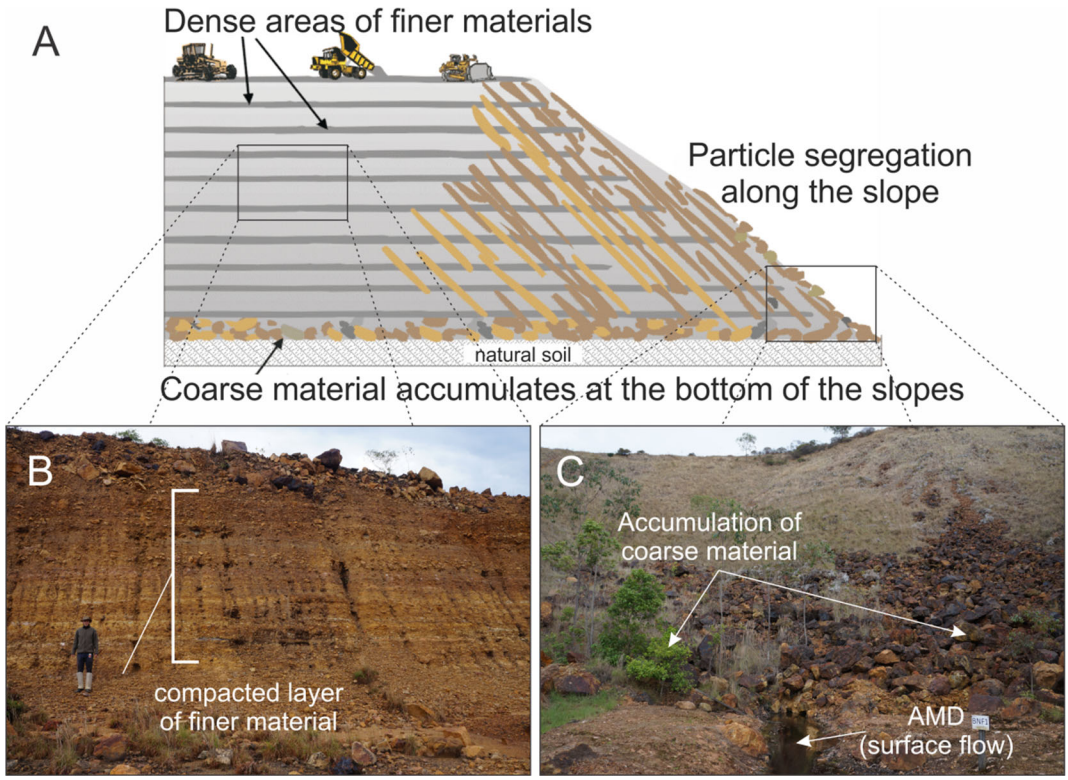

Figure 3
a Generic model of internal structure of a waste pile, according to Fala et al. (2003), and its similarity to BF-04. The pictures below indicate compacted layers composed by fine particles (**b**) and accumulation of coarse grain material at the main slope toe (**c**)

time-domain (mV/V) IP surveying or frequency-domain (ms) IP surveying (Kearey et al. 2002).

Metallic polarization is a mechanism of Induced Polarization that occurs when positives and negatives charges temporary concentrate on metallic minerals surface, whose phenomenon is directly proportional to mineral grains dissemination (Vogelsang 1995). Another polarization mechanism consists of electrolytic polarization, which is most pronounced in the presence of clay minerals. The passage of current through a rock as a result of an externally imposed voltage is accomplished mainly by electrolytic flow in the pore fluid. Most of the rock-forming minerals have a net negative charge on their outer surfaces in contact with the pore fluid and attract positive ions onto this surface. This net of ions moves to opposite directions and provides a resistance to ions flow, an effect known as membrane. Negative and positive ions thus build up on either side of the blockage and, on removal of the impressed voltage, return to their original locations over a finite period of time causing a gradually decaying voltage (Lowrie 2007; Kearey et al. 2002).

This paper chose the Electrical Resistivity Tomography technique to measure resistivity and chargeability parameters. This technique provides good results related to lateral variability of these physical parameters, which is performed by moving electrodes along the acquisition line for a two-dimensional survey. Inversion models provided conditions for the interpolation of 2D tomography lines, whose final product were multi-level surface maps and isovalue models (Pyrcz and Deutsch 2014).

Fieldworks were carried out on November during rainfall season in Poços de Caldas region. A total of 11 lines were distributed along the lower level of BF-04, a critical area that most contribute to AMD and comprises the thickest layer of the waste pile (up to 70 m). The acquisition lines were managed to reach all the waste pile geometry, with length of 400 m for

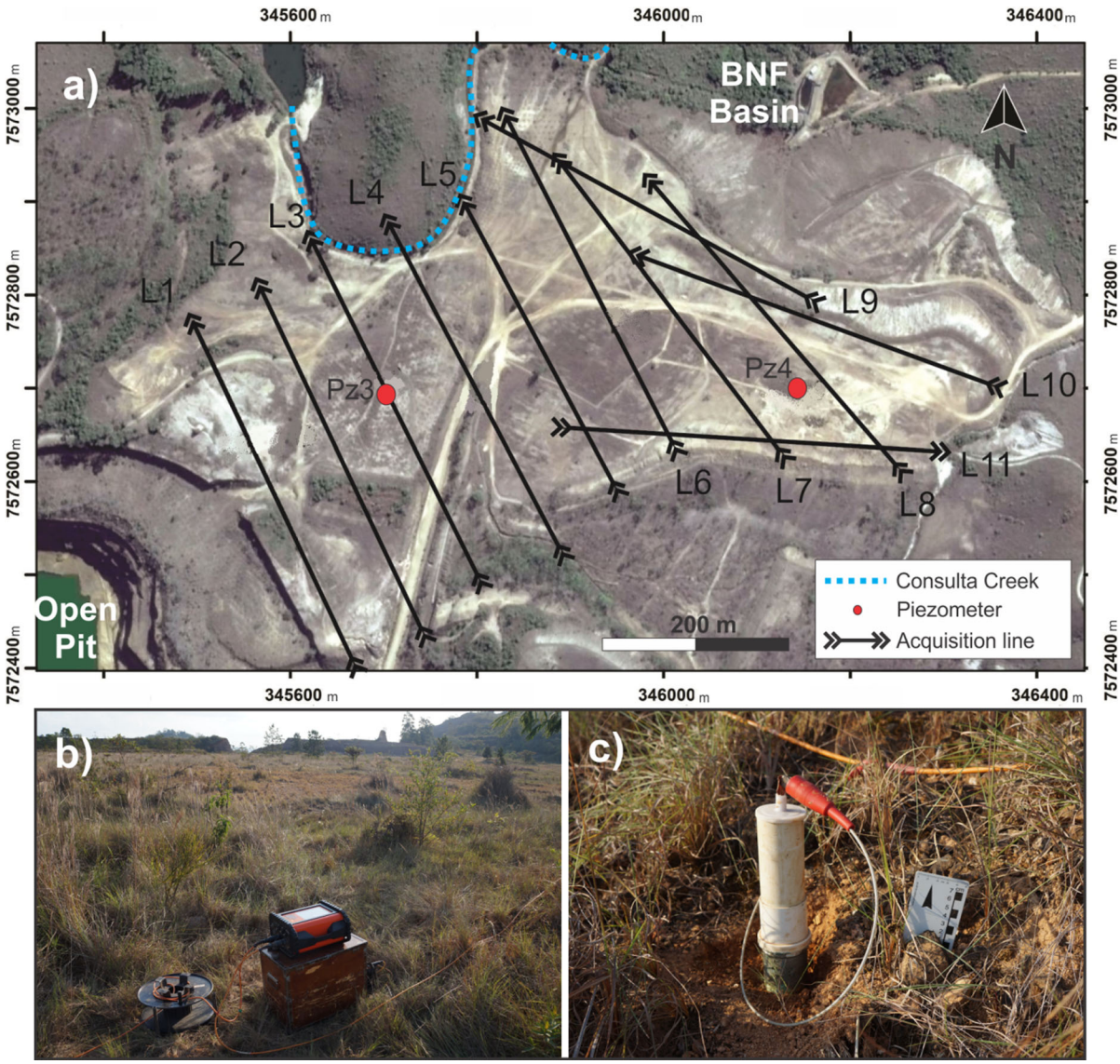

Figure 4
Disposal of geophysical lines along the lower level of BF-04 and the piezometers 3 and 4 location (**a**); ABEM Terrameter LS resistivity meter (**b**); Permeable porcelain electrodes (**c**)

each line, except line 5 with 350 m, and electrode spacing of 10 m (Fig. 4a).

The equipment used was an ABEM Terrameter LS resistivity meter with 84 channels and 250 W, maximum current of 2.5 A, resolution of 1.0 μV, and setting system to automatic acquisitions (ABEM 2012) (Fig. 4b). To proceed with the geophysical survey, it was established an electric current of 1 A, acquisition time of 1.5 s, time measurement after current cutoff of 0.3 s and readings in two time intervals with 0.1 s each, defined by preliminary tests.

Permeable porcelain electrodes with $CuSO_4$ solution were used instead of metallic electrodes, because metallic materials could generate local polarizations that would interfere in the measurement of chargeability during IP survey (Fig. 4c).

The Wenner–Schlumberger array was chosen due to its high sampling density and good horizontal and vertical resolutions. Its geometric disposal is characterized by a pair of potential electrodes fixed at the central point of the array, with a constant spacing, whereas a pair of current electrodes are placed at the edges of the tetrahedral system (Milson 2003; Knodel et al. 2007).

Res2Dinv (2D) Software 3.53 version (Geotomo Software) was used for data processing, considering topographic variations. Inversion models are represented as 2D colored sections with a chromatic logarithmic scale range. This software is designed to invert field data according to the mathematical optimization of least-squares in order to smooth extreme values (Loke and Baker 1996; Loke 2010; Bania and Cwiklik 2013).

After 2D inversion, the data were gathered in single file, later used as a database for generating multi-level surface maps and isovalue models. This process was developed in the Oasis Montaj platform, where the 2D data obtained with Res2Dinv were interpolated and modeled using the minimum curvature method for enhancement of the extreme values, in block models, where the ERT lines were positioned.

Finally, the geophysical models of BF-04 hydrogeological system were produced using the Oasis Montaj Platform (Geosoft), where data sheets from the inversion models were uploaded and interpolated based on the kriging and minimum curvature methods in order to smooth the extreme values and to reduce differences between the measured and modeled parameters.

The generation of multi-level maps and isovalue models provided conditions for a better understanding of geological structures and complex hydrogeological systems, like spreading patterns of contamination plumes and geometry of ore deposits (Chambers et al. 2006; Aizebeokhai et al. 2011; Helene et al. 2016; Moreira et al. 2016, 2018; Vieira et al. 2016).

5. *Results and Discussion*

The inversion models obtained indicated RMS error varying from 1.6 and 18.6, with average value and standard deviation of 6.34% and 5.54%, respectively. Electrical resistivity measurements indicated anomalous results that were relatively common in the study area, with resistivity values lower than 10.0 Ω m and extremely high values over 12.000 Ω m. The inversion models related to IP also provided contrasting values, whose extremely chargeability values varied from < 0.5 to > 10.1 mV/V.

Comparing these two physical parameters from the 22 inversion models, it was possible to define three groups of resistivity and chargeability anomaly sets (Table 2). Group 1 showed high resistivity values (> 1.583 Ω m) spatially related to extremely high chargeability measures (> 10.1 mV/V), which is clearly illustrated at the final edge of inversion model from acquisition line 1 (Fig. 5). This geophysical line almost covers all the BF-04 rock basement, whose thickness of waste material is insignificant at this specific location. The anomalous zones were considered as sulfides accumulation associated with resistive minerals from the rock basement, given its proximity to the open pit area and, consequently, to reliquary mineralized bodies. The fractured/weathered basement presented a resistivity range from 209 to 1.583 Ω m, whereas other inversion models indicated values higher than 12.000 Ω m for unaltered rocks.

At depth around 40 m, there is a blue colored zone characterized by relatively low values of electric resistivity, lower than 75.8 Ω m. This anomaly was linked to saline effluents, probably associated with generation and transport of AMD, due to meteoric water infiltration/runoff water, sulfides oxidation and migration towards deeper layers.

Critical areas impacted by AMD were characterized by extremely low resistivity values (< 10 Ω m). These results are compatible to Anterrieu et al. (2010) and Power et al. (2018), considering a context of waste and tailing piles affected by AMD processes. Likewise, the values of chargeability related to metallic minerals were very similar to those observed by Santos (2017) and Power et al. (2018).

Group 2 presents the most interesting set of anomalies for AMD generation, with high values of chargeability (> 10.1 mV/V) and low resistivity measures (< 75.8 Ω m). This association is a

Table 2

Characterization and interpretation of the three groups of resistivity and chargeability anomalies of BF-04 hydrogeological system

Groups	Intervals	Description
Group 1	High resistivity (> 1583 Ω m) High chargeability (> 10.1 mV/V)	Sulfide zones associated with the presence of resistive minerals (high resistivity anomalies). In most cases, the Group 1 was correlated with the underlying bedrock
Group 2	Low resistivity (< 75.8 Ω m) High chargeability (> 10.1 mV/V)	Disseminated sulfide minerals located in saturated zone of the BF-04 granular aquifer system (affected by AMD). This group is the most important because it configures the main areas undergoing oxidation process and AMD generation. Even though the pyrite concentration in the waste material comprises just 2% of it, the presence of such group of anomalies suggests portions where this reactive sulfide is relatively more abundant
Group 3	Resistivity values ranging from 10 to 1583 Ω m Low chargeability (< 10.1 mV/V)	Zones with significantly lower pyrite concentrations based on the decreasing of chargeability values. In shallow levels of the waste pile those anomalies could be understood as completely oxidized regions, where the generation of AMD is practically absent. Those low values chargeability anomalies are related to both bedrock and waste rock pile

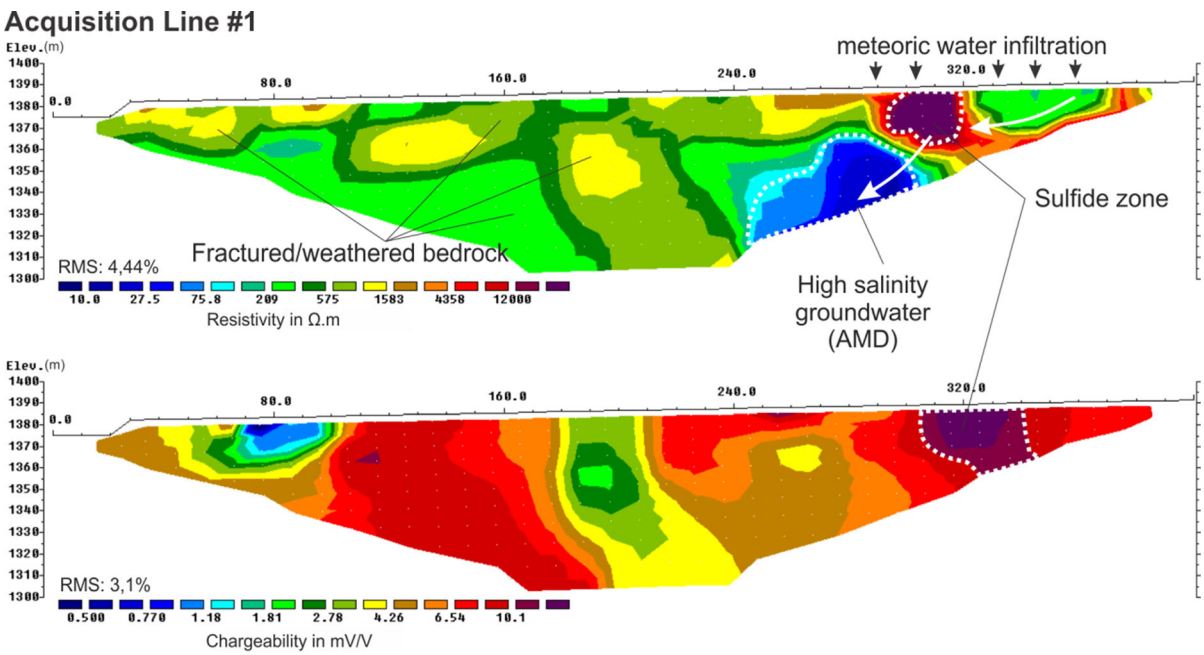

Figure 5
Resistivity (above) and chargeability (below) inversion models from line 1. Dashed lines highlight relevant anomalies and the arrows indicate groundwater flow

common feature inside BF-04 pile and understood as zones with disseminated sulfide impacted by AMD, easily distinguished in the inversion model of Line 5 (Fig. 6). Saturated zones are represented by dark shades of blue, whose central point reaches resistivity values around 10 Ω m and it is related to sulfide zones with high chargeability values (> 10.1 mV/V). On the other hand, lighter colors (from 75.8 to 100 Ω m) indicate water flows with normal hydrochemical parameters expected from an unaltered aquifer.

This low chargeability zone is a feature that goes towards Consulta Creek, indicated by several inversion models whose final edge ends close to this water stream. This fact provided some evidences about the contribution of Consulta Creek's water to generate

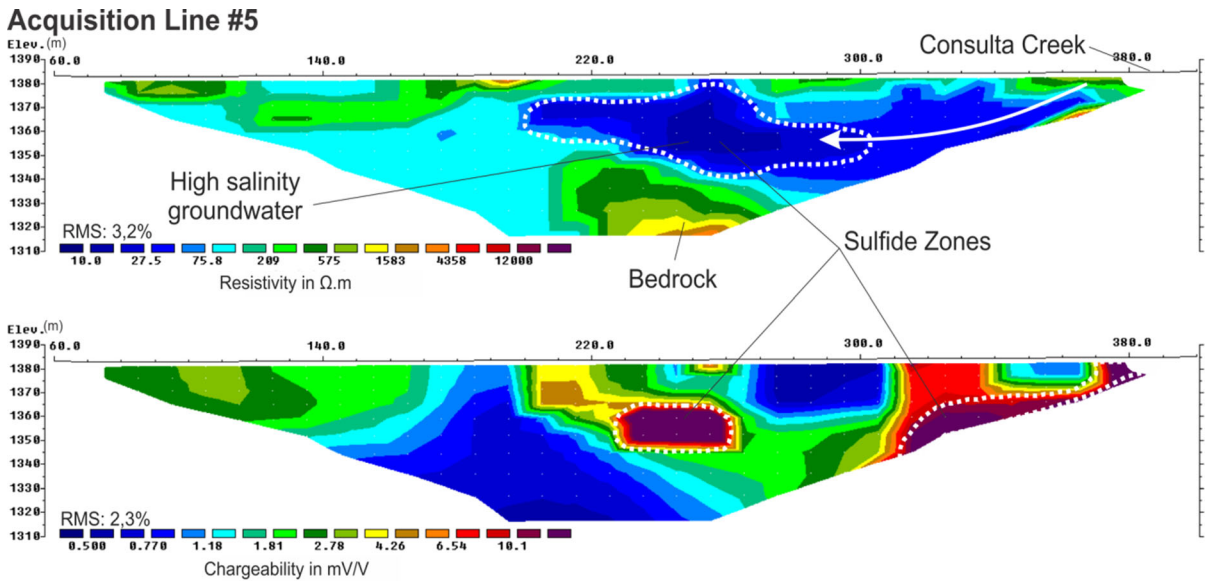

Figure 6
Resistivity (above) and chargeability (below) inversion models from line 5. Dashed lines highlight relevant anomalies and the arrows indicate groundwater flow

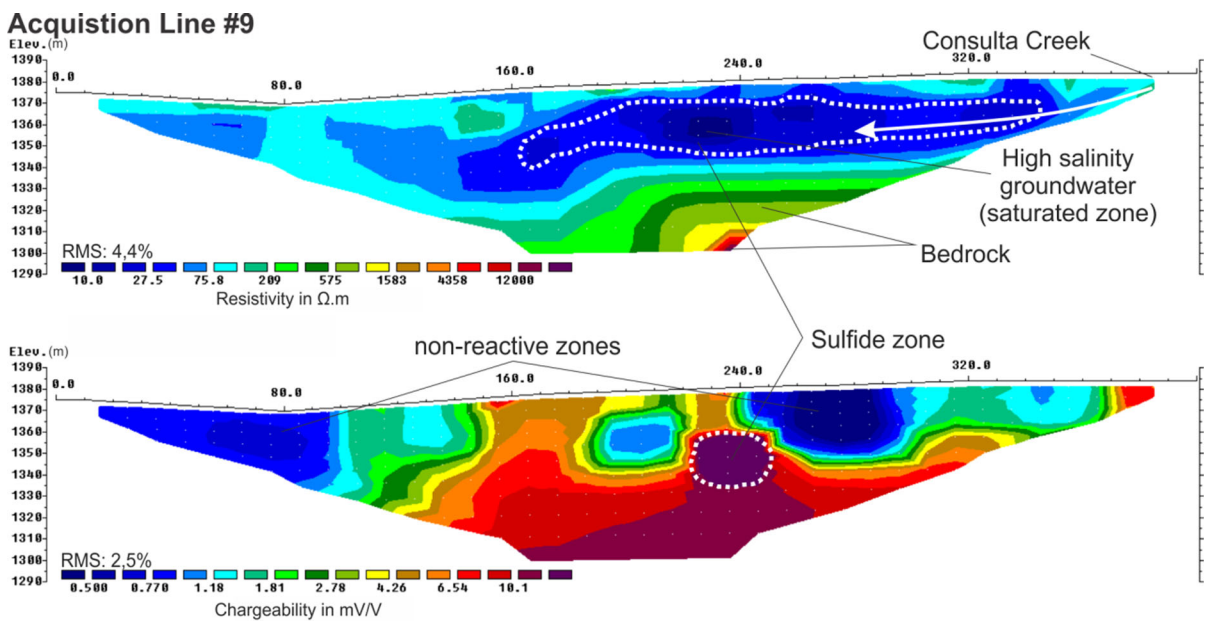

Figure 7
Resistivity (above) and chargeability (below) inversion models from line 9. Dashed lines highlight relevant anomalies and the arrows indicate groundwater flow

AMD inside the waste-rock pile. A similar context was observed at inversion models of Line 9 (Fig. 7), with bigger saturated zones due to groundwater convergence at this particular area of BF-04, close to BNF basin.

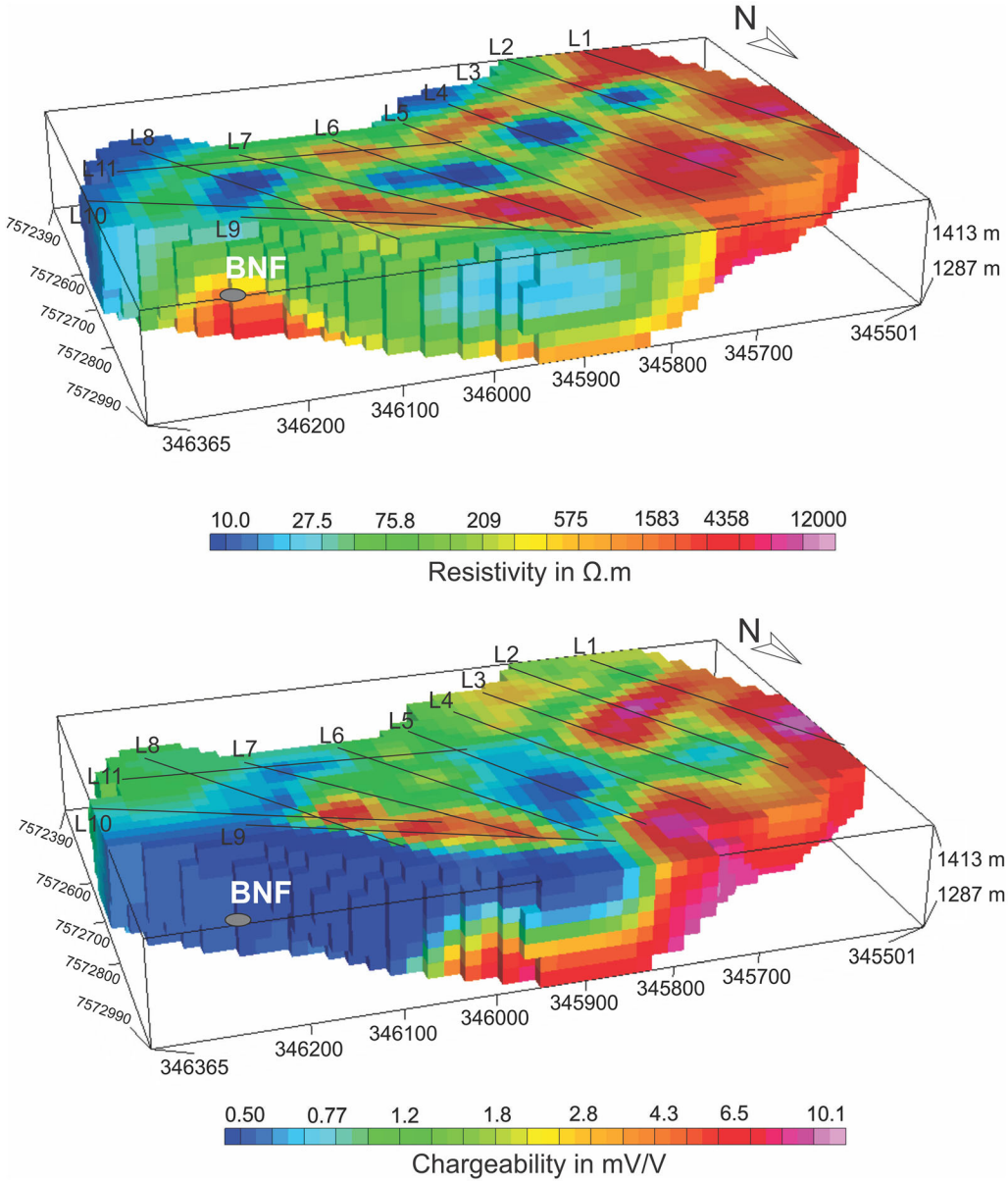

Figure 8
Resistivity and chargeability view models using kriging method

On the other hand, lower chargeability zones (< 10.1 mV/V) were identified near the surface level, both at the beginning of Line 9 and at a distance about 280 m. These zones are part of Group 3 and they are composed by relatively inert waste material considering pyrite concentration, sulfide oxidation process and AMD generation. Due to its proximity to the main slope, it is possible that atmospheric oxygen flowed easily through this surface and provided conditions to oxidize these particular zones, even though reactive sulfide core still resist in this environment.

The inversion models proved to be important tools to understand the main anomalies sets associated with BF-04 structure and AMD saturated zones. However, their limitations prevent a complete analysis of the

local hydrogeological system and the contamination mobility inside the waste pile. Thus, it was necessary to create visualization products from the interpolation of all physical parameters measured by 2D-models, even though the efficiency of the generated multi-level maps and isovalue models might be influenced by the distance between acquisition lines and edge effects.

One of the processing steps includes the creation of a block model (Fig. 8) that gives an idea of the spatial distribution of anomalous zones along superficial and lateral faces, according to acquisition lines disposal. The model was divided into 9 viewing levels considering an elevation range from 1380 to 1300 for a more accurate characterization (Figs. 9, 10).

As the waste-rock pile base is limited between 1330 and 1320 m, anomalous zones with high resistivity ($> 1583\ \Omega$ m) and chargeability (< 10.1 mV/V) values are related to the rock basement (Figs. 9, 10), whose values increase as depth increases too. At shallower levels, values higher than $4358\ \Omega$ m are easily noticeable at west and northwestern portions, because waste material thickness is smaller at these locations and basement rocks interfere on the geophysical model.

Superficial levels also provided low resistivity anomalies with a circular shape ($\sim 10\ \Omega$ m) aligned to each other that formed a continuous structure with a NE–SW trend (elevation range from 1.380 to 1.370 m). This structure is associated with an underground flow impacted by AMD, whose origin is located between lines 1 and 2 and flows to northwestern portion towards BNF basin.

This underground flow remains right below the surface, but its rectilinear shape gives way to a sharp curve towards the edge of BF-04 close to Consulta creek (1.360 m elevation). As the depth increases, the low resistivity anomaly becomes bigger and it follows, through a new curve of 45°, a subparallel path to the main slope until its disappearance at depths lower than 1320 m. This level is compatible to a region where contaminated water springs appear at the slope base, whose water is channeled towards BNF basin.

Piezometers 03 and 04 provided a good correlation between chemical analysis and geophysical anomalies indicated by the interpolation models. Piezometer 03 presents hydrochemical parameters compatible to water flows impacted by AMD, even though it was not installed at critical AMD zones (low resistivity anomalies). However, at 1360 m elevation, it seems to have a subordinated flow with smaller dimensions that pass through the piezometer. On the other hand, piezometer 04 was placed at a region with high resistivity values at deeper levels, where the absence of AMD flows would explain the lower level of contamination. All these factors corroborate to the preferential and chaotic flow model inside BF-04, caused by the physical heterogeneity of the pile and its complex hydrogeological system (Fala et al. 2003; Anterrieu et al. 2010).

Low resistivity anomalies produced edge effects on the model at south and east portions and, hence, they were not considered as AMD underground flow zones. More detailed studies are required to properly characterize such anomalies and to confirm if they are really AMD flows.

About the high chargeability anomalies (> 10.1 mV/V), they form concentrated zones both in the basement and in the waste rock material. For the purpose of sulfide oxidation and generation of AMD, the most critical areas would be those where there is the association of these anomalies with low resistivity zones, defined as Group 2. In this case, isovalue surfaces models were created according to resistivity and chargeability parameters in order to spatially delimit anomalous zones (Fig. 11).

Among the surfaces of electrical resistivity isovalues, defined by values lower than $20\ \Omega$ m, one stands out by its big dimension near to Consulta creek (northern portion). Its elongated geometry both in depth and laterality and spatial location are compatible to underground flows possibly supplied by water infiltration provided by Consulta Creek. This contribution is a key factor to understand how AMD works and to manage mitigation solutions. Besides, the shallower underground flow is also observed in isosurface model by blue semi spheres at BF-04 center region.

On the other hand, the biggest sulfide mineralization is characterized by chargeability values higher than 9.0 mV/V, defined by pink surfaces, whose origin is related to the rock basement of BF-04

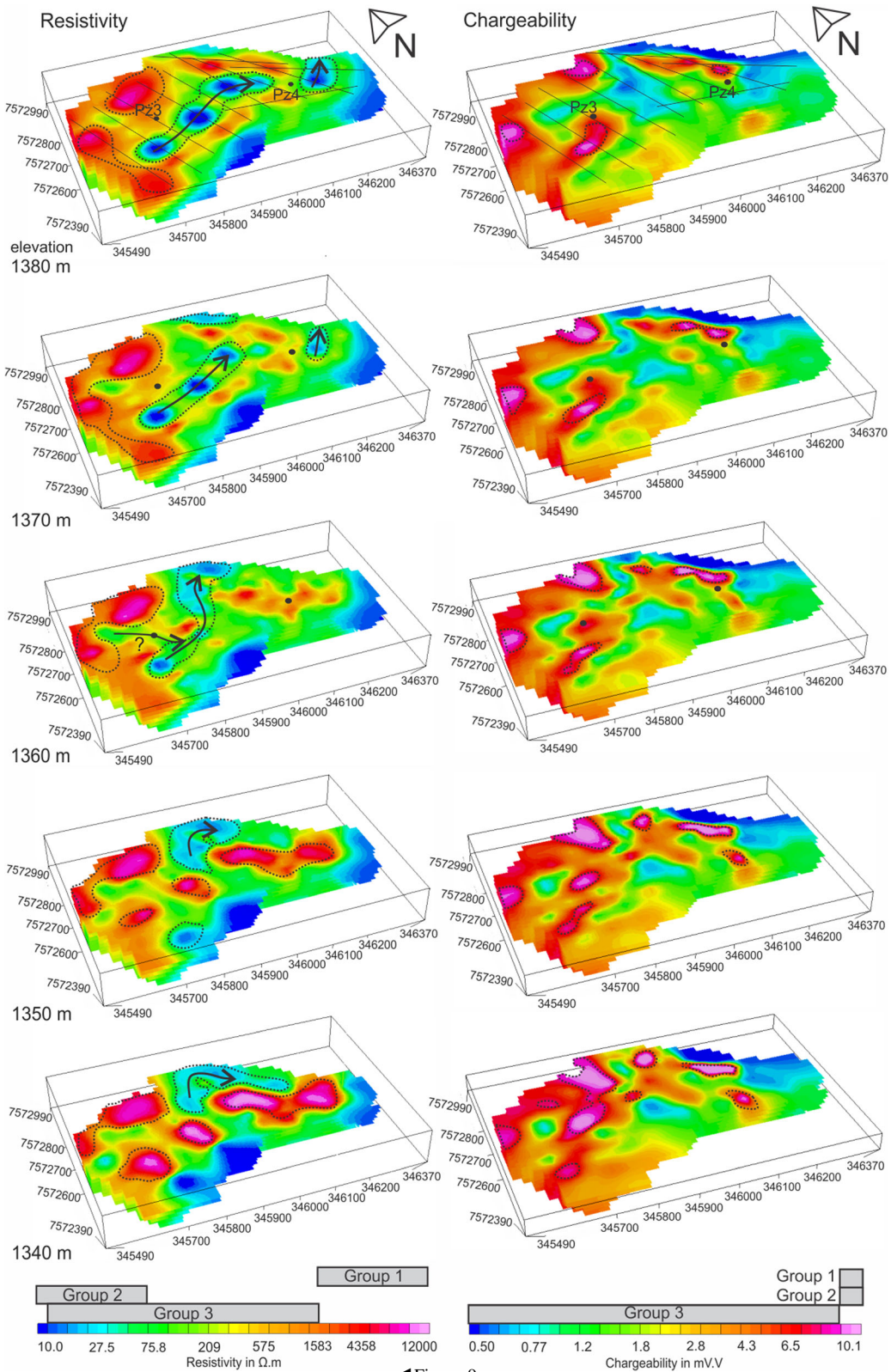

◀Figure 9

Multi-level maps (from 1395 to 1347 m) with piezometers location, hydrogeological flows and acquisition lines

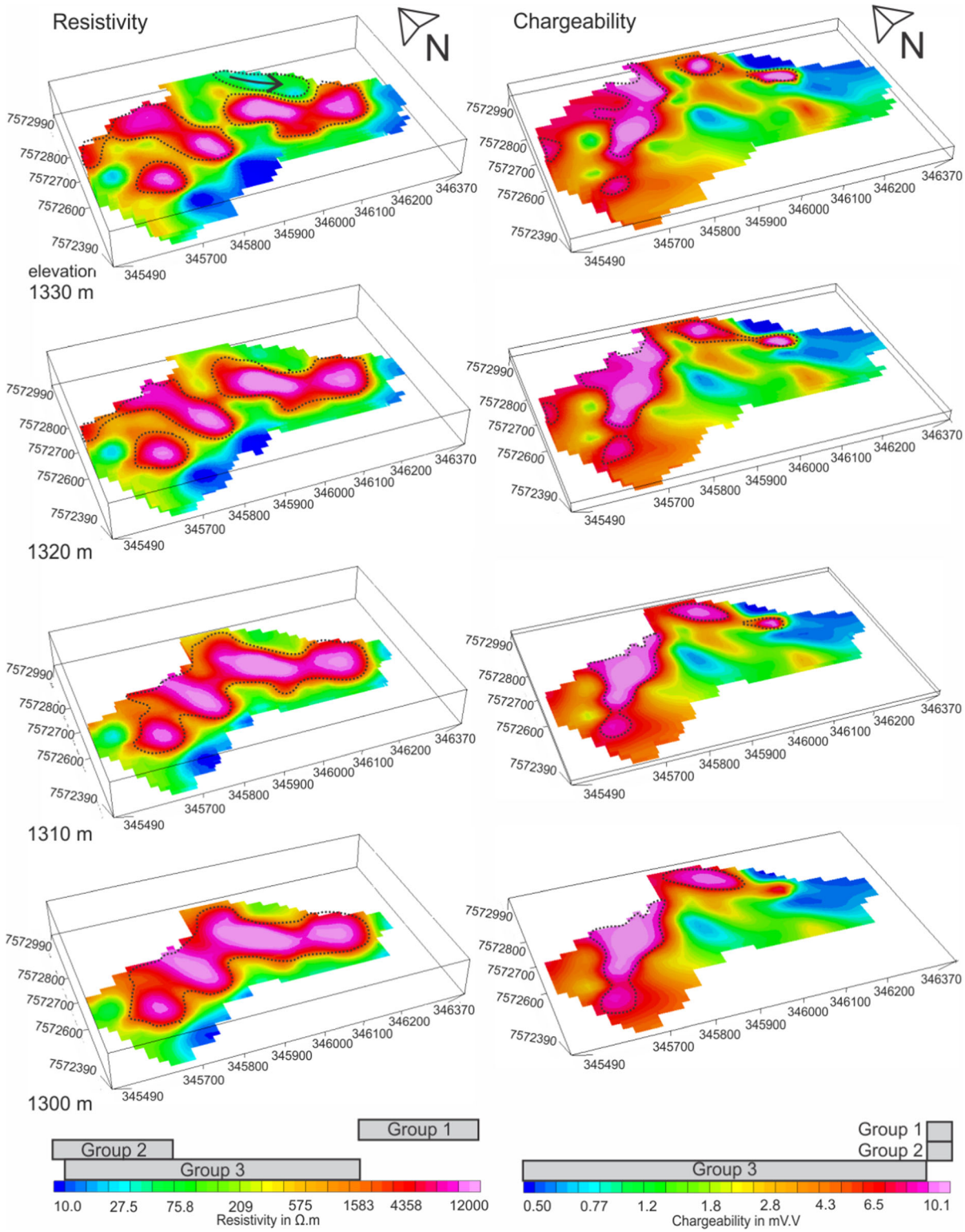

Figure 10
Other multi-level maps (from 1335 to 1299 m) with piezometers location, hydrogeological flows and acquisition lines

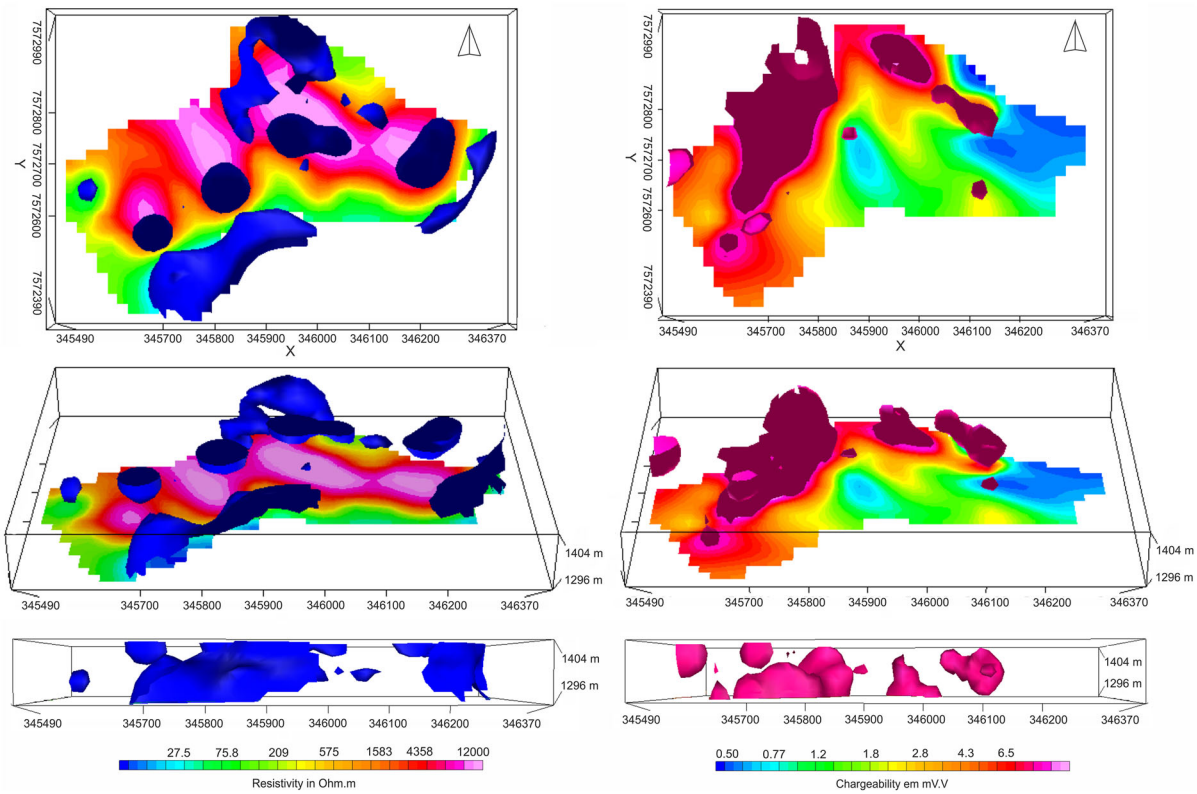

Figure 11
Isovalue surface models of resistivity (blue color, with values $< 20\ \Omega$ m) and chargeability (pink color, with values > 9 mV/V) with their respective base map corresponding to the last elevation of multilevel model

because it is located at a region with thinner layer of waste material compared to its dimensions. Other several minor sulfide mineralizations were identified inside BF-04 and classified as critical area to generate AMD.

All of these resistivity and chargeability isovalues surfaces were combined in a single model, which made it easier to stablish the correlation between the anomalies of these physical parameters (Fig. 12). The highlighted areas, named as A, B and C, have the highest potential to sulfide oxidation, water infiltration and, hence, environment contamination of BF-04. Areas that showed low resistivity values and high chargeability anomalies is a classic example of Group 2, which indicate a source of oxidation processes and the beginning of contaminated underground flows, located near the surface at the southeast portion of the waste pile.

Area B corresponds to a region where Consulta creek's water infiltrates into the pile, where there is also minor sulfide zone that certainly contributes to AMD. Area C is relevant because it is located near to the main slope surface, a place where sulfide minerals are more exposed to atmospheric air that can contribute to oxidation process (Alberti 2017).

The presence of sulfate zones related to the rock basement seems to have less influence on the generation of AMD when compared to those present inside the waste rock pile. Two examples are indicated at eastern and northeastern regions of Fig. 12, where there is only a small sulfide zone related to the formation of saline effluent, whereas the other large isosurface does not have low resistivity anomalous associated with its chargeability values higher than 9 mV/V.

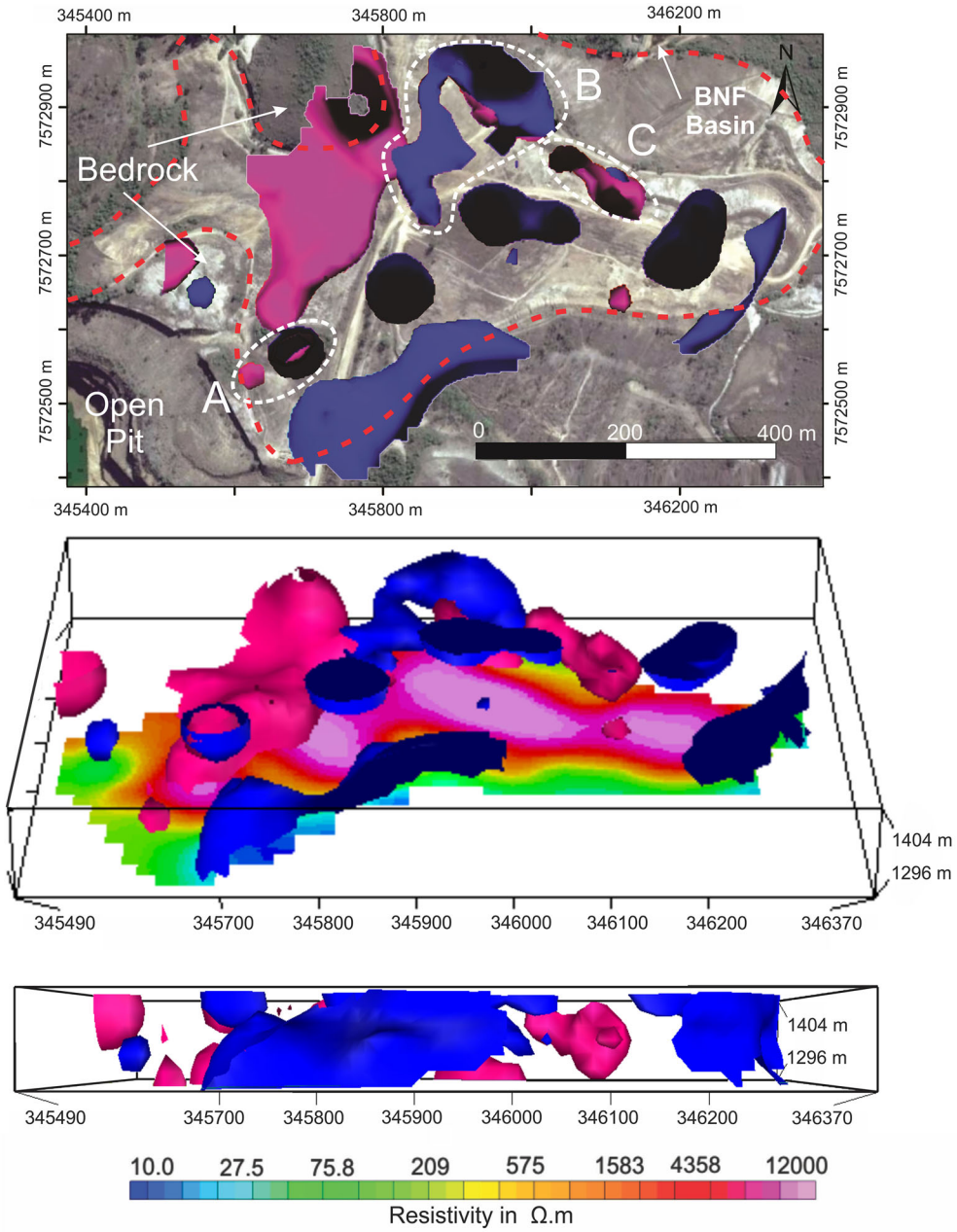

Figure 12
Isovalue surface models of resistivity (blue color, with values $< 20\ \Omega$ m) and chargeability (pink color, with values > 9 mV/V) with base map corresponding to the last elevation of multilevel model of electrical resistivity

6. *Conclusions*

Geophysical survey proved to be an excellent tool to understand dynamic processes of underground flows impacted by AMD and to identify reliquary sulfide mineralization as a potential source of contamination in waste pile. Data inversion and creation of multi-level and isovalue surface models made possible to identify anomalies associated with AMD (resistivity values lower than 75 Ω m with critical

areas of 10 Ω m) and uncontaminated groundwater. Likewise, sulfide zones with high chargeability values (higher than 10.1 mV/V) were identified both in the rock basement and within waste material. The correlation between resistivity and chargeability stablished three different setting groups and a better understanding about physical and hydrological behavior of the hydrogeological system of BF-04, as well as generation and transport of AMD.

The results demonstrated how groundwater flow is complex within artificial granular aquifer, conditioned by its granulometric and lithological heterogeneities and the presence of compacted waste material. Underground flows were observed at several depth levels including areas close to Consulta Creek's valley, which intensely contributes to water infiltration into BF-04. However, rainfall is the main water supply that reaches the waste-rock pile, whose shallow groundwater flows towards great depths into BF-04. Thus, mitigation measures must focus on waterproofing the old valley of Consulta Creek and the surface of BF-04 in order to reduce the generation of acid effluents.

The identification of AMD zones can contribute to environmental recovery and management at a detailed scale on critical areas, either by removal of reactive minerals or in situ remediation techniques, as waterproofing surfaces in order to avoid sulfide oxidation. However, it is important to notice that such mitigation actions aim just to reduce, at different scales, the AMD generation, whose occurrence will remain for several decades due to the permanent presence of dispersed grains of pyrite throughout the waste material within BF-04. In addition, it is important to emphasize that any taken environmental recovery action would begin to be effective just after 2 or 3 months due to the water residence time in the BF-04 hydrogeological system.

This study provided valuable and original data to Brazilian Nuclear Industries—INB mainly to mitigate environmental liabilities, which is an essential process of decommissioning stage in mining complexes. The integration between DC resistivity and IP methods can also be applied to waste piles from Cu, Pb, Zn, Au and coal mines associated with sulfide minerals.

Acknowledgements

The authors are thankful to São Paulo Research Foundation (FAPESP), for the financial support whereby process number 2018/14565-3 (Regular Project), the Applied Geology Department of UNESP—Rio Claro for the availability of the geophysical equipment and the Brazilian Nuclear Industries (Indústrias Nucleares do Brasil-INB) for the provided access to the study area.

References

ABEM. (2012). *Terrameter LS—Instruction manual* (p. 122). Sundbyberg: ABEM Instrument AB.

Aizebeokhai, A. P., Olayinka, A. I., Singh, V. S., & Uhuegbu, C. C. (2011). Effectiveness of 3D geoelectrical resistivity imaging using parallel 2D profiles. *International Journal of the Physical Sciences, 6,* 5623–5647.

Akcil, A., & Koldas, S. (2006). Acid mine drainage (AMD): Causes, treatment and case studies. *Journal of Cleaner Production, 14*(12), 1139–1145.

Alberti, H. L. C. (2017). Estudo hidroquímico e isotópico das águas subterrâneas impactadas pela drenagem ácida da mina de urânio—Osamu Utsumi, Planalto de Poços de Caldas (MG). Masters Dissertation—Universidade Estadual de Campinas, Campinas, p. 194.

Anterrieu, O., Chouteau, M., & Aubertin, M. (2010). Geophysical characterization of the large-scale internal structure of a waste rock pile from a hard rock mine. *Bulletin of Engineering Geology and the Environment, 69,* 533–548.

Bania, G., & Cwiklik, M. (2013). 2D electrical resistivity tomography interpretation ambiguity—Example of field studies supported with analogue and numerical modelling. *Geology, Geophysics & Environment, 39*(4), 331–339.

Belmonte-Jiménez, S. I., Jiménez-Castañeda, M. E., Pérez-Flores, M. A., Campos-Enríquez, J. O., Reyes-López, J. Á., & Salazar-Peña, L. (2012). Characterization of a leachate contaminated site integrating geophysical and hydrogeological information. *Geofísica Internacional, 51*(4), 309–321.

Benson, A. K., Payne, K. L., & Stubben, M. A. (1997). Mapping groundwater contamination using dc resistivity and VLF geophysical methods. *Geophysics, 62*(1), 80–86.

Bermejo, J. L., Sauck, W. A., & Atekwana, E. A. (1997). Geophysical discovery of a new LNAPL plume at the former Wurtsmith AFB. *Ground Water Monitoring Remediation, 17*(4), 131–137.

Blowes. D. W. (1997). The environmental effects of mine wastes. In *Proceedings of exploration 97: Fourth decennial international*

conference on mineral exploration (Vol. 4, 887–892). Toronto: Prospectors and Developers Association.

Campaner, V. P., & Silva, W. L. (2009). Processos físico-químicos em drenagem ácida de mina em mineração de carvão. *Quimica Nova, 32*(1), 146–152.

Campbell, D. L., Beanland, S. (2001). Spectral induced polarization measurements at the Carlisle mine dump (p. 11). New Mexico: U.S. Geological Survey Open-File Report, 01-363.

Campbell, D. L., Fitterman, D. V. (2000). Geoelectrical methods for investigating mine dumps. In *Fifth international conference on acid rock drainage* (pp. 1513–1523). Denver: ICARD.

Chambers, J. E., Kuras, O., Meldrum, P. I., Ogilvy, R. D., & Hollands, J. (2006). Electrical resistivity tomography applied to geologic, hydrogeologic, and engineering investigations at a former waste-disposal site. *Geophysics, 71,* 231–239.

Cipriani, M. (2002). Mitigação dos Impactos Sociais e Ambientais Decorrentes do Fechamento Definitivo de Minas de Urânio. Ph.D. Thesis—Universidade Estadual de Campinas—Instituto de Geociências, Campinas, p. 332.

Delgado-Rodriguez, O., Florez-Hernandez, D., Amezcua-Allieri, M. A., Rosas-Molina, A., & Marin-Cordova, S. (2014). Joint interpretation of geoelectrical and volatile organic compounds data: A case study in a hydrocarbons contaminated urban site. *Geofísica Internacional, 53*(2), 183–198.

Fagundes, J. R. T. (2005). Balanço hídrico do bota—fora BF4 da mina Osamu Utsumi, INB, como subsídio para projetos de remediação de drenagem ácida. MS Dissertation, Universidade Federal de Ouro Preto, Ouro Preto, p. 121.

Fala, O., Aubertin, M., Molson. J., Bussière, B., Wilson, G. W., Chapuis, R. P., Martin, V. (2003). Numerical modeling of unsaturated flow in uniform and heterogeneous waste rock piles. In *6th international conference on acid rock drainage*, Cairns.

Fraenkel, M. O., Santos, R. C., Loureiro, F. E. V. L., Muniz, W. S. (1985). Jazida de Urânio no Planalto de Poços de Caldas—Minas gerais. In *Departamento Nacional de Produção Mineral*. Principais Depósitos Minerais do Brasil: Recursos Minerais Energéticos. Brasília: DNPM, 1, cap. 5, pp. 89–103.

Franklin, M. R. (2007). Modelagem numérica do escoamento hidrológico e dos processos geoquímicos aplicados à previsão da drenagem ácida em uma pilha de estéril da mina de urânio de Poços de Caldas, MG. Ph.D. Thesis, Universidade Federal do Rio de Janeiro, Rio de Janeiro, p. 358.

Freitas, C. M., Silva, M. A., & Menezes, F. C. (2016). O desastre na barragem de mineração da Samarco—Fratura exposta dos limites do Brasil na redução de risco de desastres. *Ciência e Cultura, 68*(3), 25–30.

Gray, N. F. (1997). Environmental impact and remediation of acid mine drainage: a management problem. *Environmental Geology, 30,* 62–71.

Helene, L. P. I., Moreira, C. A., & Carrazza, L. P. (2016). Applied geophysics on a soil contaminated site by chromium of a tannery in Motuca (SP). *Revista Brasileira de Geofísica, 34,* 309–317.

Holmes, D. C., Pitty, A. E., & Noy, D. J. (1992). Geomorphological and hydrogeological features of the Poços de Caldas caldera analogue study sites. *Journal of Geochemical Exploration, 45,* 215–247.

Kearey, P., Brooks, M., Hill, I. (2002). An introduction to geophysical exploration. In *Tradução de Maria Cristina Moreira Coelho* (1st ed., p. 429). São Paulo: Oficina de Textos.

Knodel, K., Lange, G., & Voift, H. J. (2007). *Environmental geology—Handbook of field methods and case studies* (p. 1357). Germany: Springer.

Lacaz, F. A. C., Porto, M. F. S., & Pinheiro, T. M. M. (2016). Tragédias brasileiras contemporâneas: o caso do rompimento da barragem de rejeitos de Fundão/Samarco. *Revista brasileira de saúde ocupacional, 42*(9), 1–12.

Leite, J. S. M. (2010). Previsão de drenagem ácida por meio de testes estáticos do material do bota fora da mina de Osamu Utsumi—Caldas, MG. Masters Dissertation—Universidade Federal de Ouro Preto. Escola de Minas. Departamento de Geologia, Ouro Preto, p. 59.

Loke, M. H. A. (2010). Practical guide 2-D and 3-D surveys. In *Electrical imaging surveys for environmental and engineering studies* (p. 136).

Loke, M. H., & Baker, R. D. (1996). Rapid least-squares inversion of apparent resistivity pseudosections by quasi-Newton method. *Geophysical Prospecting, 44,* 131–152.

Lopes, L. M. N. (2016). The rupture of the Mariana dam and its social-environmental impacts. *Sinapse Múltipla, 5*(1), 1–14.

Lowrie, W. (2007). *Fundamentals of geophysics* (Segunda edição ed., p. 381). Cambridge: Cambridge University Press.

Lowson, R. T. (1982). Aqueous oxidation of pyrite by molecular oxygen. *Chemical Reviews, 82*(5), 461–497.

Merkel, R. H. (1972). The use of resistivity to delineate acid mine drainage in ground water. *Ground Water, 10*(5), 38–42.

Milson, J. (2003). *Field geophysics* (p. 232). England: Wiley.

Moraes, F. T., & Jiménez-Rueda, J. R. (2008). Fisiografia da região do planalto de Poços de Caldas, MG/SP. *Revista Brasileira de Geociências, 38*(1), 196–208.

Moreira, A. C., & Braga, A. C. O. (2009). Aplicação de métodos geofísicos no monitoramento de área contaminada sob atenuação natural. *Revista Brasileira de Engenharia Sanitária e Ambiental, 14*(2), 257–264.

Moreira, A. C., Carrara, A., Helene, L. P. I., Hansen, M. A., Malagutti Filho, W., & Dourado, J. C. (2017). Electrical resistivity tomography (ERT) applied in the detection of inorganic contaminants in suspended aquifer in Leme City (Brazil). *Revista Brasileira de Geofísica, 35*(3), 213–225.

Moreira, C. A., Lapola, M. M., & Carrara, A. (2016). Comparative analyzes among electrical resistivity tomography arrays in the characterization of flow structure in free aquifer. *Geofísica Internacional, 55*(2), 119–129.

Moreira, C. A., Paes, R. A. S., Ilha, L. M., & Bittencourt, J. C. (2018). Reassessment of copper mineral occurrence through electrical tomography and pseudo 3D modeling in Camaquã Sedimentary Basin, Southern Brazil. *Pure and Applied Geophysics, 175,* 1431–1445.

Mussett, A. E., & Khan, M. A. (2000). *Looking into the earth: an introduction to geological geophysics* (p. 470). New York: Cambridge University Press.

Naidoo, S. (2017). The global context of AMD. In: *Acid mine drainage in South Africa, Springer briefs in environmental science* (pp. 9–17).

Pastore, E. L., & Mioto, J. A. (2000). Impactos ambientais em mineração com ênfase à Drenagem Mineira Ácida e transporte de contaminantes. *Revista Solos e Rochas, 23*(1), 33–56.

Pichtel, J. R., & Dick, W. A. (1991). Sulfur, iron and solid phase transformations during biological oxidation of pyritic mine spoil. *Solid Biology & Biochemistry, 23,* 101–107.

Power, C., Tsourlos, P., Ramasamy, M., Nivorlis, A., & Mkanda Wire, M. (2018). Combined DC resistivity and induced polarization (DC-IP) for mapping the internal composition of a mine waste rock pile in Nova Scotia, Canada. *Journal of Applied Geophysics, 150,* 40–51.

Pyrcz, M. J., & Deutsch, C. V. (2014). *Geostatistical reservoir modeling* (p. 449). New York: Oxford University Press.

Santos, S. F. (2017). Caracterização de ocorrência de cobre por meio de levantamento estrutural e geofísico em faixa de dobramentos na região de Caçapava do Sul (RS). Masters Dissertation—Universidade Paulista Júlio de Mesquita Filho, IGCE, Rio Claro, p. 79.

Targa, D. A., Moreira, C. A., Camarero, P. L., Casagrande, M. F. S., & Alberti, H. L. C. (2019). Structural analysis and geophysical survey for hydrogeological diagnosis in uranium mine, Poços de Caldas (Brazil). *SN Applied Sciences, 1*(299), 1–12.

Thedeschi, M. F., Vieira, P. L. N. C. R., Nomo, T. A. (2015). Projeto fronteiras de Minas Gerais: Folha Caldas/Poços de Caldas, escala 1:100.000. Universidade Federal de Minas Gerais, p. 78.

Veloso, D. I. K., Moreira, C. A., & Côrtes, A. R. P. (2015). Integration of geoelectrical methods in the diagnostic of a diesel contaminated site in Santa Ernestina (SP, Brazil). *Revista Brasileira de Geofísica, 33*(4), 667–676.

Vieira, L. B., Moreira, C. A., Côrtes, A. R. P., & Luvizotto, G. L. (2016). Geophysical modeling of the manganese deposit for Induced Polarization method in Itapira (Brazil). *Geofísica Internacional, 55*(2), 107–117.

Vogelsang, D. (1995). *Environmental geophysics: A practical guide* (p. 173). Berlin: Springer.

Yuval, D., & Oldenburg, W. (1996). DC resistivity and IP methods in acid mine drainage problems: results from the Copper Cliff mine tailings impoundments. *Journal of Applied Geophysics, 34,* 187–198.

(Received April 3, 2019, revised October 16, 2019, accepted October 22, 2019, Published online November 6, 2019)